Spatiotemporal chaos in a coupled map lattice with unstable couplings

1995 J. Phys. A: Math. Gen. 28 5257

(http://iopscience.iop.org/0305-4470/28/18/015)

J. Phys. A: Math. Gen. 28 (1995) 5257–5266. Printed in the UK

Spatiotemporal chaos in a coupled map lattice with unstable couplings

Zoltán Neufeld and Tamás Vicsek

Department of Atomic Physics, Eötvös University, Budapest, Puskin u 5–7, 1088 Hungary

Received 23 March 1995

Abstract. We study the complex spatiotemporal behaviour of a coupled map lattice with a one-humped chaotic map and an unstable Laplacian coupling. Bifurcations are numerically investigated and interpreted using low-dimensional approximations corresponding to the relevant degrees of freedom of the infinite-dimensional system. Varying the control parameter we find different phases in the chaotic domain such as localized chaos or propagating chaos, spatiotemporal intermittency and transient chaos. According to our results, unstable coupling leads to a number of new features, including the effects that (i) the first bifurcation becomes discontinuous and (ii) the chaotic regime sets in sooner than for a single map.

1. Introduction

Stochastic behaviour occurring in phenomena formally described by deterministic equations has attracted much interest recently. In particular, in turbulent flows there are mechanisms, which are only partially understood, producing complex spatiotemporal behaviour beyond a given value of some characteristic parameter.

As a simpler case, one can consider spatially homogeneous systems with complicated temporal dependence described by ordinary differential equations. From the study of simple systems of nonlinear differential equations and from various simple mappings, much has been understood about chaotic temporal behaviour. In such systems the time dependence of the quantities describing the state of the system can be very different depending on the value of some control parameters. In addition to constant, periodical, and quasi-periodical temporal dependence, random-like behaviour (called deterministic chaos) can also appear even in very simple nonlinear dynamical systems. The related theoretical results accumulated over the past two decades provide a good description of these phenomena in low-dimensional nonlinear systems [1–3].

On the other hand, when one is only interested in complex dependences in space, it is necessary to consider partial differential equations (PDEs) or various discretized models. PDEs are continuous in space, time and state variables, but because of this feature the related large scale numerical investigations are very difficult to realize. A possible alternative strategy to understanding spatiotemporal complexity is to investigate simple chaotic maps assigned to the points of a lattice and coupled together via some rule. Discrete models make the simulations easier and at the same time some general aspects of PDEs may be retained. It is widely accepted that from the study of discrete systems one can obtain useful information about the nature of processes involving complex spatiotemporal behaviour, including fluid flows and pattern formation [4].

0305-4470/95/185257+10$19.50

Coupled map lattices (CML) [5] are discrete in space and time but continuous in states. They have two basic ingredients: the local dynamics is given by (i) a nonlinear map, and (ii) a coupling term (which can be local or global). Besides the investigation of general properties, CMLs are used to simulate real systems in various fields of science including neural networks [6], population dynamics in biology [7], chemical reactions [8], phase separation [9], surface roughening [10] and many others.

The first and most widely investigated CML is the diffusively-coupled logistic map [11–15]. This type of CML is dominated by the conflict between two tendencies: the diffusive coupling tends to make the system homogeneous in space, while the chaotic map produces spatial inhomogeneity due to the sensitive dependence on the initial conditions. Thus, the interesting parameter range is where the local dynamics is chaotic, since for the parameters where the map has a stable fixed point the system tends to the trivial homogeneous state.

In this paper we study a CML where the roles among these two tendencies are changed. We assume a negative value for the coupling constant in front of the Laplacian term, enhancing the growth of small spatial inhomogeneities especially at the smallest wavelength which is limited by the cut-off due to the spatial discreteness of the system. So non-trivial behaviour—including inhomogeneous state and spatiotemporal chaos—can arise even in the parameter range where the local map exhibits convergence towards a fixed point.

The choice of this kind of coupling is partially motivated by recent interest in the so called Kuramoto–Sivashinsky equation [16, 17] in which the interaction of three terms (an unstable Laplacian, a nonlinear and a stabilizing term) results in spatiotemporal complexity. However, in this work we do not intend to model a well defined physical system; our aim is to catch some general aspects caused by the interaction of an unstable coupling and a nonlinear map.

The paper is organized as follows. In section 2 we describe the model. The route to chaos, via spatiotemporal bifurcation, is treated in section 3, different aspects of chaotic phases are studied in section 4 and we discuss our results in section 5.

2. The model

The general form of our CML dynamics on a one-dimensional lattice with diffusive coupling can be written as

$$u_i^{t+1} = f_\lambda(u_i^t) + \varepsilon \frac{f_\lambda(u_{i+1}^t) + f_\lambda(u_{i-1}^t) - 2f_\lambda(u_i^t)}{2} \tag{1}$$

where u is the state variable, i and t respectively represent the discrete spatial and temporal coordinates. In our case ε is a negative constant determining the coupling strength. We mostly study the strong coupling case with $\varepsilon = -1$.

The function f represents the local dynamics and includes a control parameter λ. When making a choice for this function we must take some precautions to avoid divergence of u to infinity. For maps like the logistic map there exists a closed interval of initial conditions which leads to finite attractors. However, when the unstable coupling is switched on, some local state variables can escape from this interval and drive the system to global divergence.

There are two possible methods to control this divergence: (i) by the restriction of the control parameters to a given interval, then the map can be a properly shifted logistic map; and (ii) by modification of the map such that it becomes bounded for all u. We choose this second possibility; however, we find the same qualitative behaviour for the first case in the allowed band. Our choice for f is a Gaussian with multiplicative control parameter

$$f_\lambda(u) = \lambda e^{-(u-1)^2/K}. \tag{2}$$

This function keeps the one-humped form of the logistic map and the exponentially decaying part ensures the dissipation in the system. We choose a K value resulting in a map having (i) a well defined hump for $u > 0$ and (ii) only one fixed point. We used $K = 0.5086$ which satisfied these criteria. In some cases we studied the effect of changing of this parameter.

In figure 1 we present the bifurcation diagram corresponding to (2) and the related Lyapunov exponent for the local dynamics, which is similar to the bifurcational sequence and chaotic bands found for the logistic map. This is not surprising since the universal properties of unimodal maps are well known. The similarity holds only for λ not too large. The chaotic motion gradually disappears and inverse bifurcations occur as λ is further increased. We suppose that this is due to the exponential decaying form of the function.

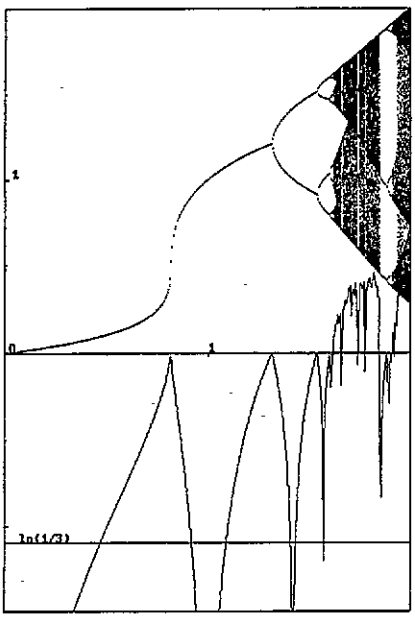

Figure 1. The bifurcation diagram (upper part) and the dependence of the Lyapunov exponent on the control parameter $0 < \lambda < 2$ (lower part) of the elementary map $f(u)$.

In our simulations we applied periodic boundary conditions and in some cases we used a random boundary condition to check the stability of the attractor. The system size was $N = 200$ and the initial conditions were random with different amplitudes distributed around the fixed point of the local map. We employed several methods for the visualization of the system's behaviour: global bifurcational diagrams, spatial distribution plots, space–time plots with system variables represented on a grey scale and first return maps.

3. The bifurcation route to spatiotemporal chaos

In this section we describe the steady state of our model as λ is increased from zero until the appearance of chaos ($\lambda \approx 0.81$).

For small λ values the only possible steady state is the homogeneous stationary state which corresponds to the fixed-point solution of the local map: $u^* = f_\lambda(u^*)$. In this interval the convergence towards the fixed point is stronger (i.e. the Lyapunov exponent is a relatively large negative number) than the effect of coupling-enhancing spatial inhomogeneities.

Depending on the initial conditions, a homogeneous ⇒ non-homogeneous transition takes place in the interval (0.42, 0.47) where the splitting of the local states into two domains creates a stationary zigzag pattern and some non-moving defects (figure 2). This splitting means that there are two disjoint intervals for u_i until large values of λ are reached. We will refer to them as the lower band (L) and upper band (U).

Figure 2. Steady state of the spatial distribution of u: zigzag patterns with defects using $\lambda = 0.65$ and system size $N = 200$.

From the linear stability analysis of the homogeneous state, we can obtain the amplification factor of small, spatially periodical perturbations with wavenumber k. Inserting

$$u = u^* + \delta u e^{ikx+\sigma t} \tag{3}$$

in (1), expanding f near u^* ($\delta u \ll 1$), and neglecting the higher order terms we obtain

$$e^{\sigma\tau} = [1 - \varepsilon(1 - \cos ka)] \left.\frac{df}{du}\right|_{u=u^*} \tag{4}$$

where τ is the time step and a is the lattice constant; both can be assumed to be equal to one in our case. This shows that the greatest amplification rate is for the perturbation with wavelength two (i.e. zigzag pattern). In accordance with (4), the homogeneous state becomes unstable ($\sigma > 0$) when the Lyapunov exponent of the local map is greater than

$$\ln\left(\frac{1}{1-2\varepsilon}\right). \tag{5}$$

This critical value is represented by a horizontal line in figure 1. When the homogeneous state becomes unstable the amplification of the zigzag pattern is saturated by the nonlinearities. The critical value in (5) is in agreement with the simulations. On the other hand, it is visible in figure 3 that the zigzag attractor already appears for some smaller λ. Thus, there exists an interval where the two attractors coexist and the steady-state depends on the initial conditions. Therefore, this is a discontinuous transition and exhibits hysteresis as can be seen in figure 3. Such hysteresis is typical for first-order phase transitions. The width of the interval where the attractors coexist is dependent on the parameter K.

In order to get an insight into the mechanism of this transition we can proceed as follows. We can simplify the situation by eliminating the defect states which lead only to local distortion of the zigzag pattern. This can be done by a properly chosen initial condition. Due to the fact that the steady state is spatially periodic, we can choose an initial condition with the same periodicity. Considering the periodic boundary condition, this system is equivalent with two coupled maps. Thus, the transition can be easily studied for two coupled maps which is a good approximation for the infinite number of coupled maps if we neglect the defect states and the distortions in their neighbourhood. The surprising similarity in the bifurcation diagram is shown in figure 4 for the two kinds of typical initial conditions (i.e. randomly distributed around the fixed point of the local map in the interval $x^* \pm 0.5$ in figure 4(*a*) and (*c*) and $x^* \pm 0.001$ in (*b*) and (*d*)). It can be seen that the branches in figure 4(*a*) and (*b*) have a fine structure that is missing in the corresponding branches in figure 4(*c*) and (*d*); this is due to the distortions in the vicinity of defects. The transition in

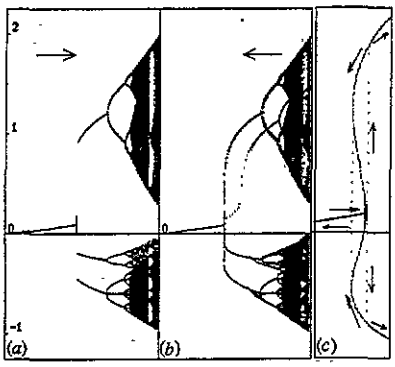

Figure 3. Bifurcation diagram for $N = 200$ with initial condition corresponding to the steady state for the previous λ. λ is increased from zero to one (*a*), and then decreased back to zero (*b*). In this way we obtained a hysteresis in the interval (0.41, 0.48). The dotted curve in (*b*) shows the unstable U defect state. In (*c*) the hysteresis cycle is magnified and completed with the unstable fixed points numerically calculated for two coupled maps.

the two-dimensional system can be studied by finding the fixed points and analysing their stability. This shows that for $\lambda > 0.42$, besides the homogeneous fixed point two other fixed points exist, one of them is stable and the other is unstable. Increasing λ, the unstable fixed point collides with the homogeneous point forming a saddle-point (figure 3(*c*)). This approximation can also be used for studying the transition where the homogeneous state loses its stability for the second time, forming zigzag patterns which oscillate in time and where a route to chaos via Hopf bifurcation occurs.

The qualitative behaviour of the defects can be well approximated with three coupled maps using the same method. In this way we obtain the fact that there can be defects both in the U and the L bands. Immediately after the transition the U defect state is unstable and for any perturbation is transformed to an L defect. At a given λ a saddle-node bifurcation takes place and results in stable U and L defects and an unstable fixed point between them, forming the basin boundary.

For λ further increased, the zigzag patterns begin to oscillate. Since the oscillations can happen in different phases, new kinds of spatial patterns appear. As can be seen in the bifurcation diagram, bifurcations in the U band are analogous to the well-known period-doubling bifurcational sequence for one dimensional maps, while the bifurcations in the L band are rather different. In order to understand this we take the following steps.

The updating rule in (1) can be separated into two terms: one depending on u_i and one depending on the neighbours (environment) of u_i:

$$u_i^{t+1} = (1-\varepsilon) f_\lambda(u_i) + \frac{\varepsilon}{2}(f_\lambda(u_{i+1}) + f_\lambda(u_{i-1})). \tag{6}$$

If u_i is in the U band the neighbours are in the L band and *vice versa*.

Let us consider the first situation: In the L band the dissipation is rather strong so that $f_\lambda(u_{i+1}) + f_\lambda(u_{i-1}) \approx$ constant, where the constant in our case is close to zero. This means that the motion in the U band can be well approximated with independent one-dimensional maps:

$$u_i^{t+1} \approx (1-\varepsilon) f_\lambda(u_i) = f_{(1-\varepsilon)\lambda}(u_i). \tag{7}$$

Thus, the bifurcational sequence is a rescaled version of that of the local maps. This is supported by the first return map at a randomly chosen position in the U band even for

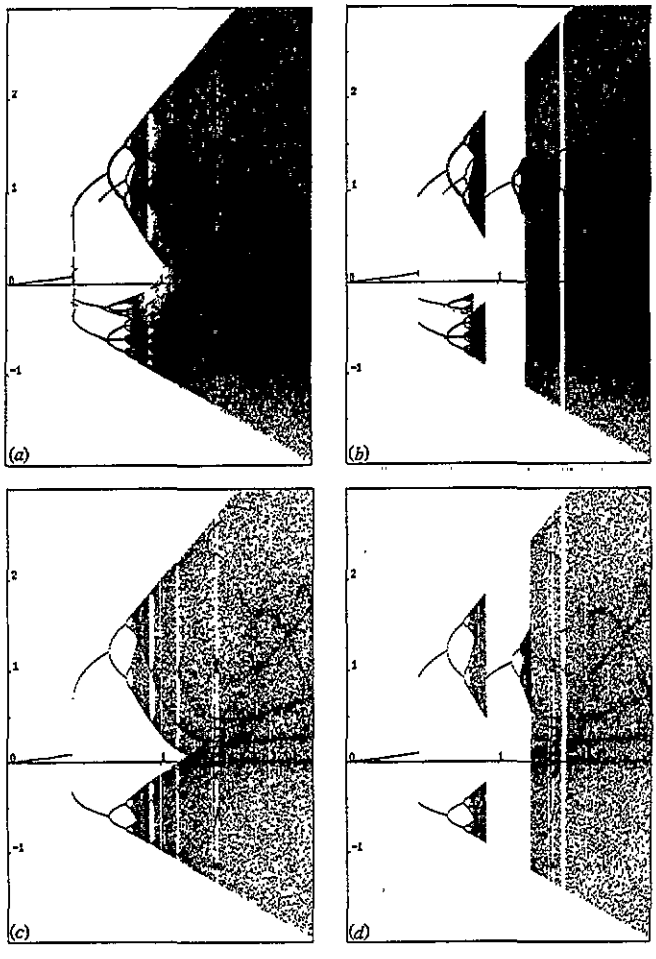

Figure 4. Bifurcation diagram for $N = 200$ ((*a*) and (*b*)), and for two coupled maps $N = 2$ ((*c*) and (*d*)) with periodic boundary conditions and λ in the interval $(0, 2)$. The initial conditions were randomly distributed around the fixed point of the local map in the interval $x^* \pm 0.5$ in (*a*) and (*c*), and $x^* \pm 0.001$ in (*b*) and (*d*). For each value of λ after the initialization, 500 iterations were performed and the u values corresponding to the last 50 iterations are plotted. In (*a*) and (*b*), u is plotted for each of the $N = 200$ sites, while in (*c*) and (*d*) u is given for $N = 2$.

λ in the chaotic domain (figure 5). When u_i is in the L band the first term is inactive ($\mathrm{d}f/\mathrm{d}x \ll 1$), but the second term oscillates in time. Thus, the bifurcations here are induced by the U band bifurcations. The difference in the diagrams is due to the fact that the oscillations of two neighbours can be in many different phases. If (i) in the U band a bifurcation takes place and u_{i+1} and u_{i-1} oscillate synchronously before bifurcation, and (ii) u_{i+1} and u_{i-1} fall in opposite phases of this new bifurcation, then the period of their induced oscillation will be half their original period (appearance of three branches). In the next bifurcation this feature does not hold because the neighbours are not in synchronous motion before the new bifurcation, and the period of the oscillation for this state is not doubled but increased by a factor of four (ramifications with four branches) (figure 6). The higher-order bifurcations do not follow this rule exactly because our approximation becomes less accurate as λ and the widths of the bands increase.

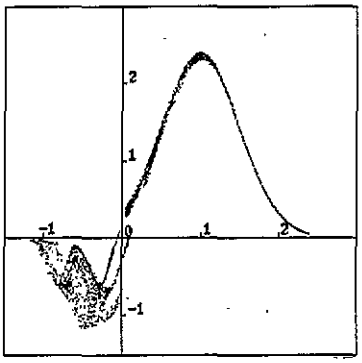

Figure 5. First return map for two typical neighbouring lattice points, one of them in the U band, and the other in the L band.

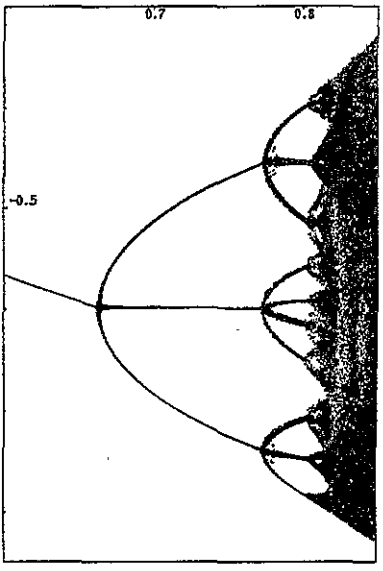

Figure 6. Bifurcation in the L band—magnification from figure 4(*a*). The same conditions were used as those described in the caption of figure 4(*a*) with the modification that the random initial conditions were chosen not to produce defect states.

Generally, when in the U band there is a 2^n-periodical motion, in the L band there exists one 2^{n-1}-periodical and 2^{n-1} 2^n-periodical states which can also have different phases. This description can be easily generalized for systems of more then one dimension where the larger number of neighbours allows more complex situations.

4. Spatiotemporal chaos

As λ is increased, beyond the accumulation point of bifurcations chaotic motion sets in the system. However, there remain some spatiotemporal regimes which are not involved in this behaviour and exhibit periodical behaviour. The structures composed by these turbulent and laminar domains lead to different phases which we present in this section.

In the first phase the chaotic motion is localized to some fixed domains. If the homogeneous state is unstable, only the defect states and their combinations can have periodic behaviour resulting in small periodical patterns. When the homogeneous attractor exists again (i.e. the Lyapunov exponent is less then $\ln(1/(1-2\varepsilon))$ for the local map), there are domains where $u_i \approx u^*$ and these domains are fixed in space, resisting the chaotic perturbations at the domain walls. The spatial distribution and the relative weight of the two kinds of domains depend on initial conditions, and the transients are very short. This kind of chaotic phase can be seen in figure 7(*a*) ($\lambda = 0.87$).

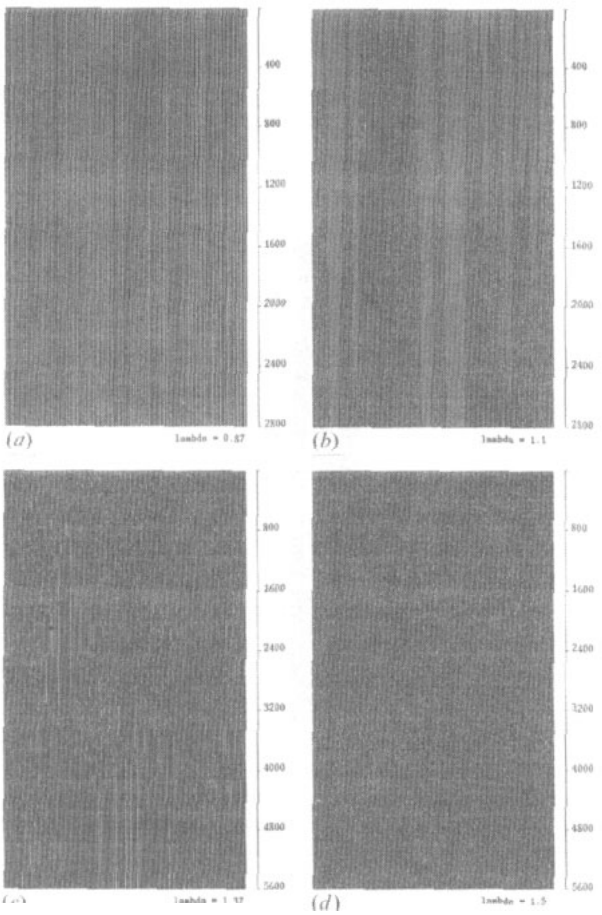

Figure 7. *Space–time plots for different values of* λ. *The spatial* direction is horizontal, the temporal direction is vertical, and U is represented on a grey scale. Every 8th ((*a*) and (*b*)) and 16th ((*c*) and (*d*)) iteration is plotted; thus periodic motion with period not larger then 8 or 16, respectively, appears as a fixed point.

For λ larger than a given value, the chaotic domains can slowly propagate into the periodic or stationary domains until they disappear, so they become just transients in this phase. Also in this phase, motion of the defect states becomes possible. The transition is continuous which means that near the transition point the propagation is very slow. (figure 7(*b*), $\lambda \approx 1.1$).

For λ further increased, the next novelty is the formation of non-chaotic domains at random places with very different sizes and lifetimes (figure 7(*c*), $\lambda = 1.37$). However,

due to the fact that these domains can be drawn to chaos just on the boundaries, it is clear that larger domains have longer lifetimes. This kind of behaviour, called spatiotemporal intermittency, has been found in various models [11, 18]. The tendency to build-up large non-chaotic domains depends on λ, so for some λ the non-chaotic domain can percolate over rather large systems falling on the periodic attractor, but chaotic transients can exist for a very long time. It seems that for a given λ there exists a characteristic length in the system which could be defined as a maximal or typical size of the laminar domains and this quantity diverges at a critical value of λ.

When λ is increased further, only chaotic motion is present and without any visible structure (figure 7(*d*), $\lambda = 1.5$). This phase can be considered as an analogue of fully developed turbulence.

5. Discussion

In this paper we have investigated a CML with an unstable coupling controlled by a nonlinear map. We have found that the locally non-chaotic elementary maps can exhibit chaos induced by the unstable coupling. In contrast to the diffusively coupled case [11, 13], the discontinuous transition to the inhomogeneous state leads to a stationary (non-oscillating) pattern. This is true for the Rayleigh–Bénard instability in fluids and also for the solution of the Kuramoto–Sivashinsky equation. The inhomogeneity generated by this splitting results in further temporal bifurcations. The transition can be studied by two coupled maps representing the relevant degrees of freedom.

The fact that one of the bands falls onto the strongly dissipative part of the map leads to extreme situations which can be used for approximations and helps us to understand the bifurcation diagram: (i) a quasi-one-dimensional map implies that the motion is not affected by the neighbours (the well-known period doubling bifurcations) and (ii) if the motion is entirely determined by the motion of the first neighbours this implies a complex bifurcational sequence.

Thus, the route to chaos is rather different in this model from those found in the diffusively coupled case.

The chaotic phases have similarities with those found in the diffusively coupled case, but there are also some differences. The localized chaos phase is similar to the frozen random phase, but there is no pattern selection phase. Instead, we find a rather large interval where in the chaotic phase non-chaotic domains with different sizes continuously appear and disappear. This phenomenon was called spatiotemporal intermittency and was related to the periodic windows in the local dynamics in the diffusive case [11]; however, in our model the local map is in a strictly non-chaotic domain. The mechanisms which are responsible for this kind of behaviour are not yet completely understood, although some similarities with the directed percolation problem have been pointed out [18].

Acknowledgments

The authors are grateful to I Jánosi and T Tél for helpful discussions. This research was supported by the Hungarian Research Foundation grant No T4439 and by the EEC Human Capital Mobility Programme contract No ERB-CHRX-CT92-0063.

References

[1] Schuster H G 1988 *Deterministic Chaos* (VCH)
[2] Marek M and Schreiber I 1991 *Chaotic Behaviour of Deterministic Dissipative Systems* (Cambridge: Cambridge University Press)
[3] Ott E 1993 *Chaos in Dynamical Systems* (Cambridge: Cambridge University Press)
[4] Cross M C and Hohenberg P C 1993 *Rev. Mod. Phys.* **65** 851
[5] Kaneko K 1992 *Chaos* **2** 279
[6] Nozawa H 1992 *Chaos* **2** 377
[7] Csilling Á, Jánosi I M, Pásztor G and Scheuring I 1994 *Phys. Rev.* E **50** 1083
[8] Levine H and Reynolds W N *Chaos* **2** 337
[9] Oono Y and Puri S 1986 *Phys. Rev. Lett.* **58** 836
[10] Pikovsky A S and Kurths J 1994 *Phys. Rev.* E **49** 898
[11] Kaneko K 1984 *Prog. Theor. Phys.* **72** 480; 1985 *Prog. Theor. Phys.* **74** 1033
[12] Kaneko K 1986 *Physica* D **23** 436
[13] Kaneko K 1989 *Physica* D **34** 1
[14] Willeboordse F H 1993 *Phys. Rev.* E **47** 1419
[15] Kaneko K 1994 *Physica* D **77** 456
[16] Sivashinsky G I 1977 *Acta Astronaut.* **4** 1177
[17] Kuramoto Y 1978 *Prog. Theor. Phys. Suppl.* **64** 346
[18] Chaté H and Manneville P 1988 *Physica* D **32** 409